International Journal of Mass Spectrometry 280 (2009) 190–197

Contents lists available at ScienceDirect

International Journal of Mass Spectrometry

journal homepage: www.elsevier.com/locate/ijms

Fragmentation of deprotonated D-ribose and D-fructose in MALDI—Comparison with dissociative electron attachment

Ilko Bald[a,b,*], Helga D. Flosadóttir[a], Janina Kopyra[b,c], Eugen Illenberger[b], Oddur Ingólfsson[a,*]

[a] University of Iceland, Department of Chemistry, Science Institute, Dunhaga 3, 107 Reykjavik, Iceland
[b] Free University Berlin, Institute of Chemistry and Biochemistry – Physical and Theoretical Chemistry, Takustraße 3, 14195 Berlin, Germany
[c] University of Podlasie, Department of Chemistry, 08-110 Siedlce, Poland

ARTICLE INFO

Article history:
Received 14 July 2008
Received in revised form 20 October 2008
Accepted 8 December 2008
Available online 24 December 2008

Keywords:
Ribose
Fructose
Fragmentation
MALDI
Dissociative electron attachment
DEA

ABSTRACT

We present a detailed, collaborative study on the fragmentation of deprotonated native D-ribose and D-fructose and the isotopically labelled 1-^{13}C-D-ribose, 5-^{13}C-D-ribose and C-1-D-D-ribose. The fragmentation is studied in a matrix assisted laser desorption/ionization time of flight mass spectrometer (MALDI ToF MS), both in in-source decay (ISD) and post-source decay (PSD) mode and compared with fragmentation through dissociative electron attachment (DEA). Fragmentation of deprotonated monosaccharides formed in the MALDI process, as well as their transient molecular anions formed upon electron attachment are characterized by loss of different numbers of H_2O and CH_2O units. Two different fragmentation pathways leading to cross-ring cleavage are identified. Metastable decay of deprotonated D-ribose proceeds either *via* an X-type cleavage yielding fragment anions at m/z = 119, 100 and 89, or *via* an A-type cleavage resulting in m/z = 89, 77 and 71. A fast and early metastable cross-ring cleavage of deprotonated D-ribose observed in in-source decay is dominated by X-type cleavage leading mainly to m/z = 100 and 71. For dissociative electron attachment to D-ribose a sequential dissociation was identified that includes metastable decay of the dehydrogenated molecular anion leading to m/z = 89. All other fragmentation reactions in DEA to D-ribose are likely to proceed directly and on a faster timescale (below 400 ns).

1. Introduction

Carbohydrates are the most abundant organic compounds on earth and make up the bulk of all plant material. Examples of common monosaccharides are the aldopentoses arabinose, ribose and deoxyribose; the aldohexoses galactose, glucose, and mannose; and the ketohexose fructose. Among the disaccharides the most common are the sucrose, which is composed of fructose and glucose, the lactose, which is composed of glucose and galactose and mannose which is the hydrolysis product of the most common energy storage form in plants, starch. Starch is the most important nutrition form for human beings and mainly composed of amylopectine and amylase, which are both polymers made up of glucose units. Other common polysaccharides are cellulose, glycogen, chitin and the inuline fibers that are complex polymers of fructose units also referred to as fructans. These are also, like starch, an important form of energy storage for some plants. The individual monosaccharides can combine through glycosidic bonds between any of the hydroxyl groups or the anomeric center resulting in branched molecules of almost unlimited structural diversity.

Saccharides are also found in conjunction with or as a building block of other essential biological molecules. Glycoproteins for example are an integral part of many membrane proteins and play an essential role in the immune system. Another example are the glycolipids such as the more than 40 gangliosides which are found predominantly in the nervous system and play an important role in cell to cell communication and membrane conductance and transport. Last but not least, the monosaccharide units ribose and deoxyribose play a pivotal role as a structural element of RNA and DNA, respectively. It is thus not surprising that the scientific community has invested considerable effort in trying to understand the structure and composition of the vast variety of polysaccharides and the role of the sugars in the multiplicity of biologically relevant molecules. Mass spectrometry of sugars has been conducted with a variety of ionization methods, including electrospray ionization [1,2], direct laser desorption and matrix assisted laser desorption ionization (MALDI) [3–7], fast atom bombardment (FAB) [8–10], chemical ionization [11], field desorption [12,13], liquid secondary ion mass spectrometry [14], infrared multiple-photon dissociation [15], one-photon dissociation [16] as well as low-energy ion induced dissociation [17,18]. A number of studies have also been conducted on the fragmentation pattern of cationized sugars after

* Corresponding authors at: University of Iceland, Department of Chemistry, Science Institute, Dunhaga 3, 101 Reykjavik, Iceland.
E-mail addresses: ibald@zedat.fu-berlin.de (I. Bald), odduring@hi.is (O. Ingólfsson).

1387-3806/$ – see front matter © 2008 Elsevier B.V. All rights reserved.
doi:10.1016/j.ijms.2008.12.010

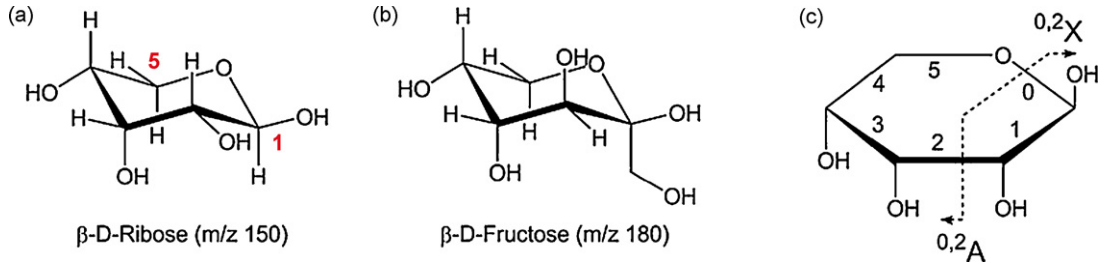

Fig. 1. Molecular structure of (a) D-ribose and (b) D-fructose. Carbon numbers 1 and 5 of D-ribose are labelled. (c) Example for notation of cross-ring cleavage according to Domon and Costello [28].

collisional activation. These include studies of monosaccharides complexed with Pb^{2+} [19,20], glucose with Cu^{+} [21] and a number of trisaccharides complexed with the alkaline earth metal ions Ca^{2+} and Mg^{2+} [22].

Furthermore, in conjunction with the potential role of low-energy electrons in the damage ionizing radiation can cause to biologically relevant molecules such as DNA and RNA [23,24] also studies on low-energy (0–20 eV) electron induced dissociation in 2-deoxy-D-ribose [25] and D-ribose [26] as well as in the hexose D-fructose [27] have been conducted. In these studies it was shown that the DNA sugar 2-deoxy-D-ribose [25] and the RNA sugar D-ribose [26] are in fact remarkably sensitive towards low-energy electrons. The same applies for the hexose D-fructose [27]. Thus the stability of the sugar unit may play a crucial role when biological material is exposed to high-energy radiation through which low-energy electrons are produced in large quantities [23,24].

Here we present a detailed, collaborative study on the fragmentation mechanism of D-ribose and D-fructose after deprotonation in MALDI, and on the other hand when the molecular ion is initially formed through the resonant attachment of a free electron with virtually no kinetic energy. In the MALDI experiments, both in-source decay (ISD) that proceeds within the first 400 ns after ionization, and post-source decay (PSD) reactions that proceed in a time window of 5–15 μs were studied. The electron attachment experiments were conducted on an electron attachment spectrometer which is described in the next section. To be able to verify the site of fragmentation and to draw conclusions about the mechanism behind the observed fragmentation patterns we conducted all experiments on the native compounds D-ribose and D-fructose and the isotope labelled compounds 1-^{13}C-D-ribose, 5-^{13}C-D-ribose and C-1-D-D-ribose. Fig. 1 shows the two compounds D-ribose (a) and D-fructose (b). The isotopically marked carbons C1 and C5 are signified for D-ribose. Throughout this paper we are using the nomenclature of Domon and Costello [28] for sugar cross-ring cleavages (see Fig. 1c for an instructive example). Furthermore we refer to $[M-H^+]^-$ for a deprotonated neutral molecule and to $[M-H]^-$ for a dehydrogenated anion. Although both species are chemically the same the different notation implicates their distinct origin.

2. Experiment

The MALDI experiments presented here were performed in Reykjavík with a REFLEX IV (Bruker Daltonics) UV-MALDI time-of-flight reflectron type mass spectrometer. The instrument and its operation in PSD mode has been described in fair detail elsewhere [29] and here we only give a short overview. The MALDI-ToF is equipped with an N_2 laser (337 nm, 200 μJ/pulse) operated with 7–10 Hz repetition rate. The ISD spectra were all recorded in reflectron mode and the laser power was set to be about 10% above the detection threshold for the deprotonated molecular ion. The PSD spectra were recorded by gating the deprotonated molecular ions into the field free linear flight tube. The desorption laser power was kept about 20% above the detection threshold for the corresponding ion and the laser spot was moved manually over the sample during acquisition to average out sample inhomogeneity. The gate width was ±5 Da in all experiments and the extraction of the ions was operated in pulsed delayed extraction mode with 400 ns delay time. The total acceleration voltage through the linear region was 20 kV resulting in about 10 μs flight time, which is the time window within which we observe metastable decay. After the linear flight the ions are decelerated and reaccelerated with a grid-less reflectron and detected on a double micro-channel plate detector. The reflectron voltage is stepped down in 7 segments to assure for collection of all fragments. Individual segments are the sum of 500 shots which are recorded by using the fragmentation analyses and structural ToF method FAST, within the instrumental control software FlexControl®. The alignment of individual segments and the mass calibration of the spectra is carried out with the FlexAnalyses® software also provided by the instrument manufacturer. Samples were prepared by pre-spotting 0.5 μL of a 2.8 mM solution of matrix (bisbenzimide; $C_{25}H_{24}N_6O{\cdot}3HCl$) in methanol on a stainless steel sample carrier. After drying the matrix in air, 0.5 μL of aqueous 0.13 M solution of D-ribose was spotted on the matrix and allowed to dry.

Dissociative electron attachment under single-collision conditions was measured in Berlin. The apparatus is described in detail elsewhere [30]. Briefly, the sample molecules are heated in a vessel to moderate temperature (<100 °C) until an appreciable anion signal is obtained. The evaporated neutral molecules cross an electron beam of defined but variable energy that is generated by a trochoidal electron monochromator. Negative ions formed by electron attachment are mass selected and detected in a quadrupole mass spectrometer as a function of the incident electron energy. The energy was calibrated using the well-known 0 eV resonance of SF_6 yielding SF_6^-. The SF_6 flow was switched off prior to each measurement in order to prevent ion-molecule reactions. In the current experiment the energy resolution of the electron beam was typically about 80–120 meV and the electron current was about 10 nA.

D-ribose, the isotope analogue 5-^{13}C-D-ribose, D-fructose and bisbenzimide were obtained from Sigma–Aldrich (stated purity 98, 99 and ≥98%, respectively), 1-^{13}C-D-ribose and C1-D-ribose were obtained from Cambridge Isotope Laboratories, Inc. (stated purity 99 and 98%, respectively). All samples were used as delivered.

3. Results and discussion

3.1. Fragmentation of deprotonated D-ribose and D-fructose in MALDI

The metastable decay spectra of deprotonated D-ribose ($[R-H^+]^-$) and D-fructose ($[Fru-H^+]^-$) obtained by MALDI-ToF are displayed in Fig. 2. Decomposition of $[R-H^+]^-$ and $[Fru-H^+]^-$ is characterized by loss of water and different numbers of formaldehyde

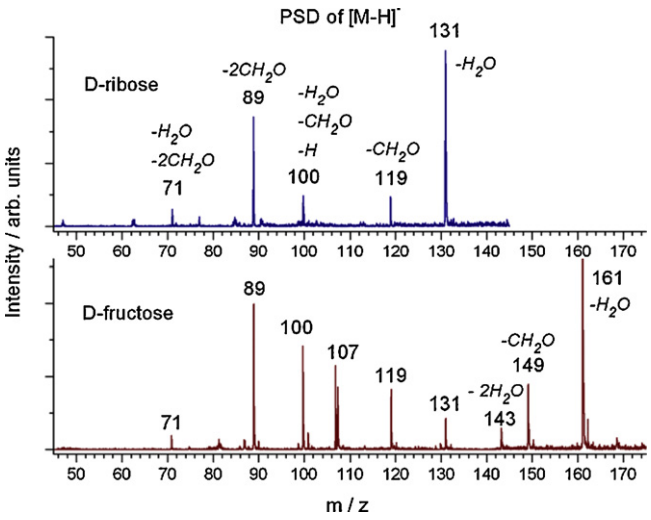

Fig. 2. Metastable decay spectra of deprotonated D-ribose (upper spectrum) and deprotonated D-fructose (lower spectrum).

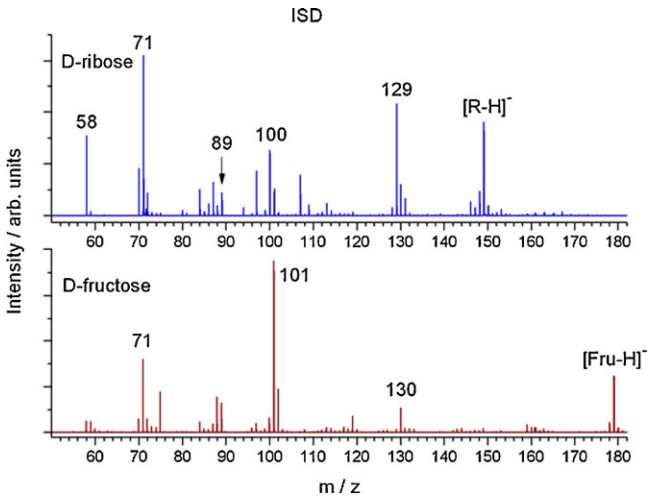

Fig. 3. In-source decay spectra of $[R\text{-}H^+]^-$ (upper spectrum) and $[Fru\text{-}H^+]^-$ (lower spectrum).

units ($m/z = 30$). This results in the following fragmentation pattern for the deprotonated D-ribose:

$$[R\text{-}H^+]^-(C_5H_9O_5^-;\ 149\,u) \rightarrow C_5H_7O_4^-(131\,u) + H_2O \quad (1)$$

$$\rightarrow C_4H_7O_4^-(119\,u) + CH_2O \quad (2)$$

$$\rightarrow C_4H_4O_3^-(100\,u) + H_2O + CH_2O + H \quad (3)$$

$$\rightarrow C_3H_5O_3^-(89\,u) + 2CH_2O \quad (4)$$

$$\rightarrow C_2H_5O_3^-(77\,u) + C_3H_4O_2 \quad (5)$$

$$\rightarrow C_3H_3O_2^-(71\,u) + 2CH_2O + H_2O \quad (6)$$

Deprotonated D-fructose shows the same fragmentation products (apart from $m/z = 77$). The most dominant fragmentation channels in metastable decay of both these molecules in MALDI are the abstraction of one water molecule from the deprotonated precursor and the formation of the $m/z = 89$ fragment anion. In comparison to D-ribose, D-fructose possesses an additional methylhydroxy group at C1 (Fig. 1). Hence, to arrive at the same m/z ratios as observed for the fragment ions from D-ribose, D-fructose has to lose an additional 30 u. In addition to the fragments listed above for D-ribose, metastable decay of D-fructose also leads to the formation of $C_3H_7O_4^-$ ($m/z = 161$), $C_5H_9O_5^-$ ($m/z = 149$), $C_6H_7O_4^-$ ($m/z = 143$), and $C_6H_3O_2^-$ ($m/z = 107$). From these, the first two correspond to loss of one water molecule ($m/z = 161$) and one formaldehyde unit ($m/z = 149$), respectively. These fragments therefore correspond to the fragments observed for D-ribose at $m/z = 131$ and 119, respectively. The fragment at $m/z = 143$ is attributed to the loss of two water molecules and represents thus a fragmentation path that we do not observe for the D-ribose. The m/z ratio 107 is most likely formed by a $^{2,5}X$ cross-ring cleavage (see Fig. 1) and a hydrogen transfer to the $^{2,5}X$ fragment. The m/z ratio could also be explained by the sequential loss of four water molecules, however this must be considered to be an unlikely event. Correspondingly a $^{2,5}X$ cleavage in D-ribose results in the fragment ion at $m/z = 77$.

ISD spectra of D-ribose and D-fructose are shown in Fig. 3. For D-ribose the striking difference to the metastable decay spectra is the strong appearance of the m/z ratios 58, 71, and 129 of which $m/z = 58$ and 129 are not observed in PSD. For D-fructose the dominating ISD fragments appear at the m/z ratios 71 and 101 of which the 101 u fragment is the more intense. Neither the mass 58 nor 129 u is observed with any appreciable intensity from D-fructose. However a comparably intense signal is observed at 88 u which might correspond to the m/z ratio 58 from D-ribose with the methylhydroxy group attached. Also a relatively intense signal is observed at 130 u. The fragment ion at $m/z = 89$ which is by far the most pronounced fragment in PSD of both these compounds is only weakly visible in ISD. It is however not surprising that there is a considerable difference between the ISD and the PSD spectra. For one thing, the ISD takes place in the expanding plume under multiple collision conditions while PSD proceeds under collision free conditions. However, not less important is the fact that all fragment ions observed in ISD are formed within the ion source before the acceleration voltage is applied, i.e., within 400 ns. In contrast PSD spectra are recorded for the decomposition of a pre-selected precursor ion which has had about 10 μs to fragment. Consequently, formation of the ions at the m/z ratios 129, 100, 71 and 58 (in the case of D-fructose $m/z = 130$, 101 and 71) are from fast and early metastable decay (<400 ns), whereas the formation of the fragment $m/z = 89$ and the other dominating PSD fragments proceeds on a much longer time scale.

Fragmentation of some collisionally activated deprotonated pyranose monosaccharides has been studied by means of ESI quadrupole time-of-flight tandem mass spectrometry [2] and by FAB [9], respectively. Similar to ISD and PSD in MALDI both these collisional induced dissociation (CID) studies report the loss of different numbers of neutral water and CH_2O units as the typical fragmentation pattern. However, in both these investigations the m/z ratio 113 is observed for D-ribose as well as D-fructose. For D-ribose this mass corresponds to the loss of two water molecules and for D-fructose to the loss of two water molecules and a CH_2O unit. This fragment does not appear with any appreciable intensity in the ISD spectra or the PSD spectra observed here. Furthermore, in the PSD spectra reported here the m/z ratio 100 is dominant for both D-ribose and D-fructose and this is also true for the ISD spectra of D-ribose. In the CID investigation on the other hand the m/z ratio 101 is the dominating one [2]. This is also the case for ISD of D-fructose. The slightly different fragmentation products in CID compared to PSD are most likely due to the different internal energy of the precursor ion. The internal energy of an analyte ion desorbed by MALDI was determined to be below 4.3 eV [31,32], whereas the center-of-mass collision energy in Ref. [2] was 1.7 eV for an ion of $m/z = 149$ with argon as collision gas at a pressure of 0.7 bar. This high pressure in the collision cells of these experiments results in multiple collisions thereby incorporating much higher internal energy into the precursor ion than in the present MALDI–PSD experiments.

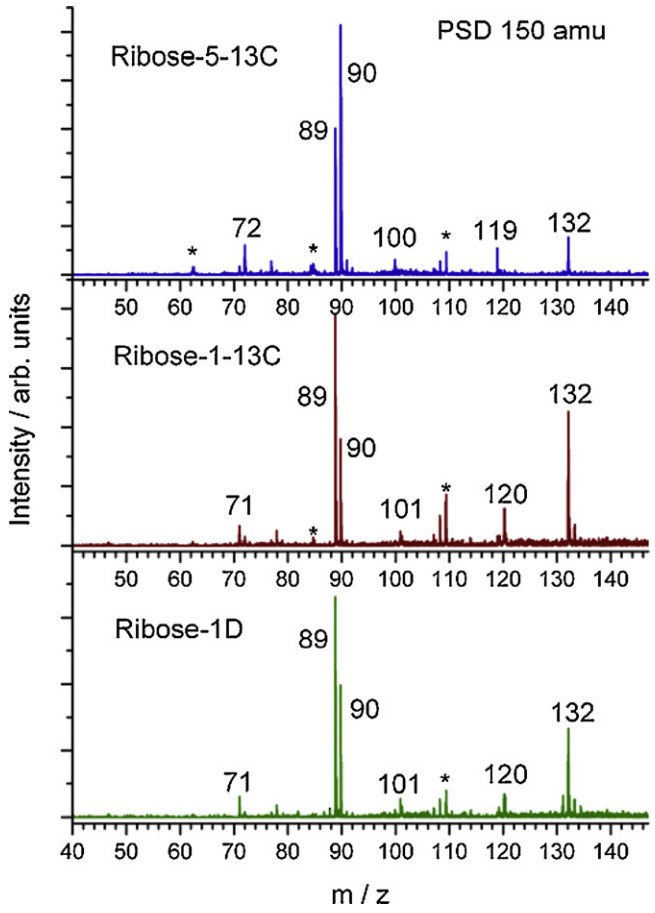

Fig. 4. Metastable decay spectra of the isotope labelled deprotonated D-ribose analogs 5-^{13}C-R, 1-^{13}C-R and 1-D-R.

3.2. Fragmentation mechanisms in post-source decay of deprotonated D-ribose

As mentioned above, the comparison of D-ribose and D-fructose shows that either ionic fragments with the same mass are observed in both molecules, or fragmentation pathways corresponding to the same neutral products (loss of H_2O and CH_2O units). Assuming that ionic fragments with the same mass are identical in both D-ribose and D-fructose the PSD fragments at m/z = 71, 89, 100 and 119 should not contain the carbon C1 since the additional mass loss from D-fructose corresponds to the loss of its additional methylhydroxy group. In other words, at first glance it is reasonable to assume that the ionic fragments that have the same m/z ratios in the PSD spectra from D-ribose and D-fructose are predominantly generated *via* an A-type cross-ring cleavage. Fragment ions on the other hand that correspond to the same neutral loss should then contain the C1 carbon as these are shifted by the mass of the methylhydroxy group (30 u) in D-fructose. It would thus be reasonable to assume that these fragments result from an X-type cleavage. However, as we will discuss below this is not the case and in fact we can show unambiguously that both the masses 100 and 119 u are formed by X-type cross-ring cleavage and thus do contain the C1 carbon. To be able to identify the fragmentation sites without any doubt we performed a detailed investigation using the isotope labelled derivatives 1-^{13}C-D-ribose (1-^{13}C-R), 5-^{13}C-D-ribose (5-^{13}C-R) and C-1-D-D-ribose (1-D-R). The corresponding PSD spectra are shown in Fig. 4.

For a complete discussion of the fragmentation pathways it is important to know where in the sugar molecule the deprotonation takes place. A proton is most likely abstracted from the most acidic hydroxyl group, which is the anomeric hydroxyl group in solvated monosaccharides. It was shown in theoretical studies of D-glucose in the gas phase that the acidity differences of the different hydroxyl groups are much less pronounced than in solution [33,34]. Depending on the theoretical method used for calculations also the OH group at C4 is predicted to have high acidity [33]. Higher level DFT calculations using extended basis sets including diffuse functions confirm that the hydroxyl group at the anomeric center of D-glucose has the largest acidity followed by the OH group at C4 [34]. Deprotonation of the anomeric OH group leads to a considerable lengthening of the endocyclic C1–O bond thus enabling a ring opening with very low activation barriers. However, the acidity difference between the other hydroxyl groups is small and the activation barriers for proton transfer between two adjacent OH groups is low, making a "proton ring walk" possible at the slightly energetic conditions [34] in MALDI. Though the calculations were conducted for D-glucose we assume that the same applies for D-ribose. Consequently different deprotonated species may be present in the mass spectrometer.

The PSD spectra of the three different isotope labelled D-ribose molecules are shown in Fig. 4. As expected for the loss of one water molecule the peak at m/z = 131 is shifted to m/z = 132 independent of the ^{13}C site. In 1-D-R however, a small contribution remains at m/z = 131 suggesting that some water molecules are also generated *via* C1–D and C–OH bond cleavage. Alternatively to a C–H(D) and C–OH elimination a water molecule may be generated from D-ribose by C–OH and CO–H bond cleavage. It is however more likely that the abstraction proceeds *via* the loss of a carbon bound hydrogen along with a hydroxyl group, but if there is a preferable site for the elimination it cannot be determined from the current data. Water loss from hexoses has been proposed to proceed from the closed ring structure [9]. However, elimination from the open chain structure is favoured since the free rotation of the C–C bond enables the formation of a periplanar geometry that is preferred in an E2 elimination [35]. Furthermore, the acidity of the C2 hydrogen is increased in the open chain, where it is located in α position of the carbonyl group (see Fig. 6). Thus water elimination from the C2–H and C3–OH should be the most favourable site.

The PSD spectra of isotope labelled D-ribose (Fig. 4) show that the signal at m/z = 119, that corresponds to the loss of a single CH_2O unit, is not shifted to m/z = 120 in 5-^{13}C-R. Conversely it appears exclusively at m/z = 120 in 1-^{13}C-R and C-1-D-R. The neutral CH_2O unit is thus exclusively composed of C5 and the negative charge remains on the C1 site, i.e., the fragment with the m/z ratio 119 is exclusively formed through a ^{0,4}X cross-ring cleavage. The same exclusive selectivity is observed for the fragment anion m/z = 100. It is thus most likely also generated through a ^{0,4}X cross-ring cleavage, but with additional loss of H_2O and H to form a radical anion.

Fig. 5 shows a proposed fragmentation mechanism for the main fragments observed in PSD of the deprotonated D-ribose. Starting from the ring opening of $[R\text{-}H^+]^-$ a cleavage of the C4–C5 bond results in CH_2O formation with the negative charge on C4. A proton transfer leads to a stabilization of the fragment anion with mass 119 hence representing a ^{0,4}X cleavage. It was also proposed previously that formation of m/z = 119 is due to deprotonation at the C2–OH and concerted ring opening leading to an epoxy-like structure (with abstraction of C5) [9]. Such a mechanism leads to the same site selectivity as observed here, but most likely requires the surmounting of high activation barriers [34].

For the m/z = 89 fragment anion, which dominates the PSD spectra of D-ribose, the site selectivity is considerably less pronounced than in the case of the fragments at m/z = 119 and 100. About 2/3 of the signal at m/z = 89 is shifted to m/z = 90 in 5-^{13}C-R. Conversely, in 1-^{13}C-R 2/3 of the signal remain at the m/z ratio 89. This is also true for 1-D-R. Thus 2/3 of the fragmentation leading to m/z = 89 is

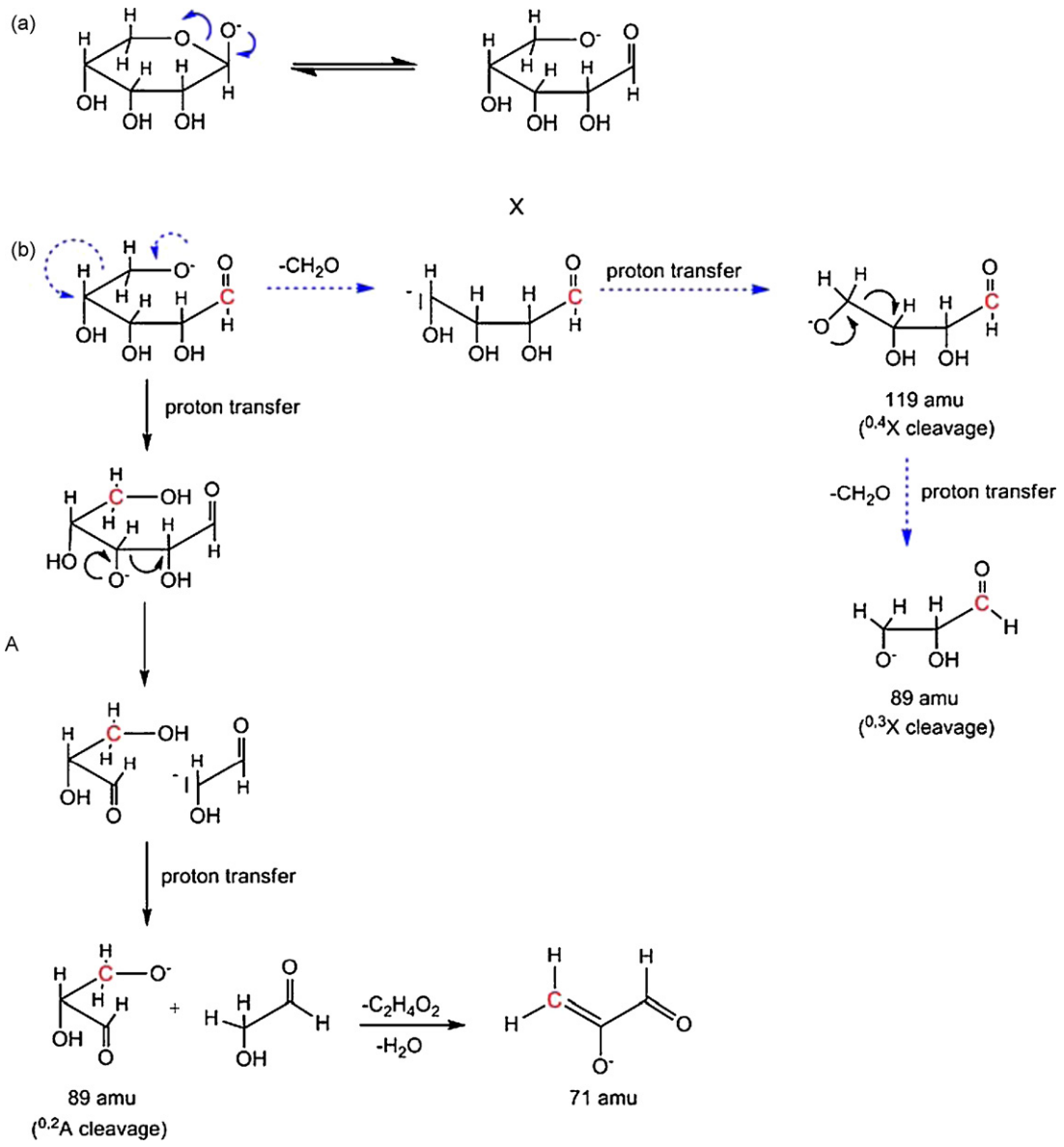

Fig. 5. Reaction scheme showing (a) the ring opening of D-ribose deprotonated at the anomeric hydroxyl group, and (b) the two different reaction sequences (X and A) yielding the m/z = 119, 89 and 71 anions.

concordant with a ^{0,2}A cross-ring cleavage. However, the remaining 1/3 of the signal that is shifted to m/z = 90 in 1-^{13}C-R (and remains at m/z = 89 in 5-^{13}C-R) cannot be explained in this way. An additional mechanism leading to the m/z ratio 89 with the negative charge remaining on the C1 containing fragment must therefore be operative, hence a ^{0,3}X cleavage. This is similar to the reaction leading to the loss of a single CH_2O unit (m/z = 119). Fig. 5 shows the paths for the formation of the fragment m/z = 89 as it would result from a ^{0,3}X and a ^{0,2}A cross-ring cleavage, respectively. In both cases the initial step is the ring opening. For the ^{0,2}A cross-ring cleavage the ring opening is followed by a proton transfer from the hydroxyl group at C3 and a subsequent C–C bond cleavage leading to the abstraction of a $C_2H_4O_2$ unit as was previously suggested by Carroll et al. [36]. In the case of the ^{0,3}X fragment on the other hand the abstraction of one formaldehyde unit and subsequent proton transfer first leads to the fragment m/z = 119 as described above. A subsequent loss of the C4 formaldehyde unit then leads to the formation of the ^{0,3}X fragment at the m/z ratio 89. The close resemblance of the spectra of 1-^{13}C-R and 1-D-R indicates that the hydrogen bound to C1 is not involved in this reaction. In a recent CID study of deprotonated D-glucose complexed with Pb^{2+} (resulting in [Pb(D-glucose)-H]$^+$) using electrospray ionization [20] the elimination of $C_2H_4O_2$ (m/z = 60) was also found to be the most dominant fragmentation reaction. By means of different isotope labelled D-glucose molecules the loss of neutral $C_2H_4O_2$ was unambiguously assigned to arise exclusively from C1 and C2. This corresponds to the ^{0,2}A elimination mechanism shown in Fig. 5. In PSD of "bare" deprotonated D-ribose this fragmentation channel also dominates, but additionally the ^{0,3}X cleavage is operative. This is not surprising as the difference between metastable decay of deprotonated monosaccharides and collision induced dissociation of cationized monosaccharides is considerable and also obvious when looking at the other fragments generated. In the present study the loss of one water molecule is a dominant reaction and the loss of a single formaldehyde unit is also observed with appreciable intensity. In the previously performed CID experiments of the cationized D-glucose [20], D-fructose [19] and D-ribose [19] the latter reaction is not operative at all and the former is only a minor fragmentation channel. The considerable differences to the spectra presented here can be attributed to (i) the coordination of Pb^{2+} to the sugars that

changes the reactivity of particular reactions, (ii) the different internal energy of the precursor ion in metastable decay as compared to CID, and (iii) the presence of a small fraction of the furanose form of D-ribose in the aqueous solution in ESI. It is interesting to note that the loss of a single formaldehyde molecule is usually not observed in disaccharides [2,14] and oligosaccharides [10] indicating that the X-type fragmentation is mainly operative in isolated monosaccharides.

Similar to the fragment formation at $m/z = 119$ and 100 the $m/z = 71$ fragment anion is also formed with very high site selectivity. However, this fragment which is formed by loss of H_2O in addition to two CH_2O molecules is predominantly formed through the loss of C1, and C5 remains a part of the negatively charged fragment. Hence the spectra of the isotope labelled ribose molecules indicate that the anion at $m/z = 71$ is due to additional water loss from the ^{0,2}A cleavage at $m/z = 89$ as shown in Fig. 5.

3.3. Fragmentation mechanisms of deprotonated D-ribose in in-source decay in MALDI

In Fig. 6 the ISD spectra of isotope labelled D-ribose are shown in the mass range from 50–152 u. In ISD of D-ribose the loss of H_2O ($m/z = 131$) is only a very minor contribution. However, the m/z ratio 129 which corresponds to the loss of an H_2O along with H_2 from the deprotonated D-ribose is observed with appreciable intensities. Loss of H_2 was observed previously in D-glucose complexed with Cu^+ [21], but not the loss of both H_2 and H_2O. As discussed above, the conditions under which fragment ions are formed in ISD and PSD are very different. The main difference lies probably in the fact that ISD proceeds under multiple collisions within the expansion plume and quasi equilibrium conditions may be presumed. Thus, the ISD product at $m/z = 129$ is probably simply more stable than the PSD product observed at $m/z = 131$. As expected, the complete $m/z = 129$ peak is shifted to $m/z = 130$ in 1-^{13}C-R and 5-^{13}C-R. Somewhat surprising on the other hand is that also in 1-D-R the bulk of the signal is observed at $m/z = 130$ and only a very small fraction is observed at $m/z = 129$. As half of the hydrogen atoms (5) are abstracted from the sugar to form this fragment one would expect a considerably larger fraction to be observed at $m/z = 129$ if the underlying dissociation process would be purely statistical. Thus it is obvious that this specific ISD cannel is highly site selective.

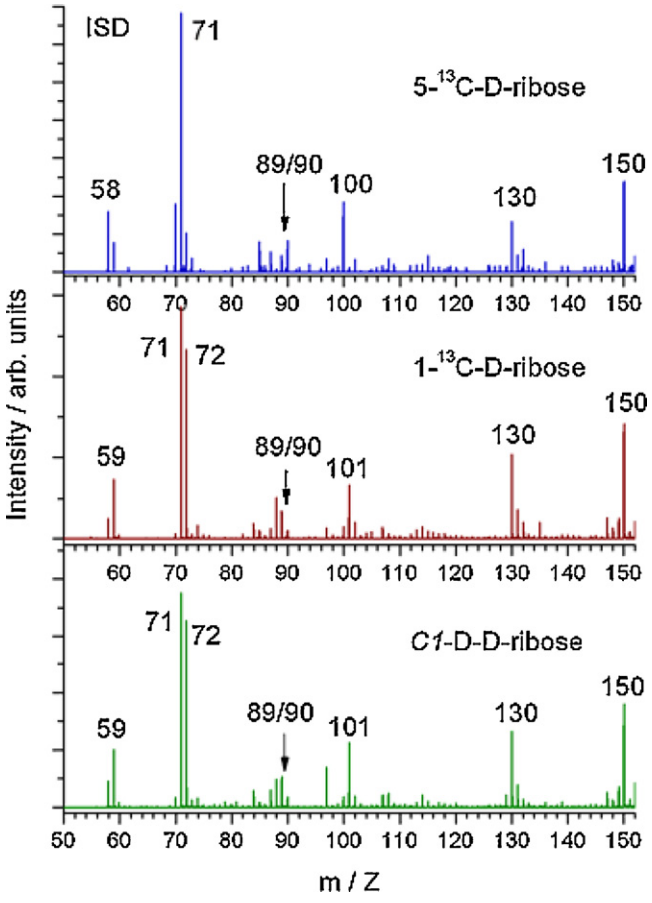

Fig. 6. In-source decay spectra of the isotope labelled deprotonated D-ribose analogs 5-^{13}C-R, 1-^{13}C-R and 1-D-R.

For the signal observed in the ISD spectra at the m/z ratio 100 the situation is somewhat different as the formation of this fragment is accompanied by the loss of one carbon atom through the extraction of a CH_2O unit. In the isotope labelled D-ribose this signal is close to being quantitatively shifted by one mass unit for 1-^{13}C-R and 1-D-R, but no shift is observed for 5-^{13}C-R. Thus the formation of this fragment can be assigned to a ^{0,4}X cross-ring cleavage like the formation of the m/z ratio 119 in the PSD spectra. However, here the cross-ring cleavage is followed by a water and a neutral hydrogen loss. This is exactly the same observation as was made for the m/z ratio 100 in PSD of the isotope labelled D-ribose. We therefore presume that in this case the same mechanism is operative in ISD and PSD. The mass spectra around the m/z ratio 71 is identical for 5-^{13}C-R and the unlabelled D-ribose, but a little bit less than half of the signal intensity is shifted to the m/z ratio 72 for 1-^{13}C-R and 1-D-R. Thus two mechanisms must be operative when this fragment is formed. Both of these mechanisms must lead to the loss of C5 but only one leads also to the loss of C1. The fragmentation must therefore proceed by the sequential loss of two CH_2O units from C5 and C1 or through a ^{0,3}X cross-ring cleavage where C5 and C4 either leave sequentially as two CH_2O units or in one step as a $C_2H_4O_2$ unit. Both mechanisms are accompanied by the additional loss of H_2O. In this case the situation is very different from what we observe for the formation of the m/z ratio 71 in PSD where we exclusively observe an A-type cleavage, i.e., in PSD C5 is always included in the negative fragment at $m/z = 71$. Finally, one can see from Fig. 6 that about 2/3 of the signal at $m/z = 58$ is shifted to $m/z = 59$ in 1-^{13}C-R and 1-D-R. Conversely, in 5-^{13}C-R 2/3 of the signal remains at $m/z = 58$. We can therefore conclude that 2/3 of the fragment intensity at $m/z = 58$ results from a ^{0,2}X cleavage but about 1/3 result from a ^{0,3}A cleavage. Furthermore, it is also clear that the hydrogen at C1 is not lost through the ^{0,2}X cleavage.

3.4. Metastable fragmentation in dissociative electron attachment to D-ribose

So far we have only discussed PSD and ISD of anions generated through deprotonation in MALDI. However, in recent experiments the Berlin group studied the fragmentation of the D-ribose radical anion generated by the resonant capture of low-energy electrons, i.e., through dissociative electron attachment (DEA). The results of these studies are discussed to a large extent in Refs. [26,37], however neither the formation of the fragment $m/z = 89$ upon DEA, which was also observed in these studies, nor the mechanism behind the formation of this fragment has been discussed. The main fragment anions formed by DEA close to 0 eV electron energy were the fragments with the m/z ratios 132, 114, 101, 102, 71, 72 and 59 [26]. These fragments as well as the fragment with the m/z ratio 89 were all formed close to zero eV electron energy. Hence the $[R]^-$ transient negative ions initially formed are formed without any excess energy beyond the electron affinity of the sugar molecule. This is very different from the situation in the MALDI process where the ions formed with close to 4 eV internal energy. As the initial molecular ions are formed in the DEA study contains very little internal energy the fragment assign-

ments made in Ref. [26] were mainly based on thermochemical considerations.

In general the fragment ions in DEA were observed one mass unit above the ones recorded in MALDI, indicating that the neutral decomposition products of $R^{\#-}$ in DEA and the anion $[R\text{-}H^+]^-$ formed through deprotonation in MALDI are mainly the same. However, fragments also appear in DEA that are not observed in MALDI. The most pronounced of these is the fragment at $m/z = 114$ in DEA [26], which might correspond to the fragment observed at $m/z = 113$ in the CID experiments discussed above. However, the generally close resemblance to the fragments observed in the present MALDI experiments and the DEA experiments suggest that the mass-to-charge ratios in both experiments correspond to the loss of the same numbers of water and formaldehyde molecules. In addition to the m/z ratios listed above also a weaker signal was observed at $m/z = 89$ in the DEA experiments. Different from the other fragments, which are all partly or fully shifted higher by one mass unit in the DEA spectra, the fragment at $m/z = 89$ appears exclusively at that mass in both experiments. In a recent study on L-valine [38] PSD of the deprotonated ion $[Val\text{-}H^+]^-$ formed in MALDI was compared to the metastable decay of $[Val\text{-}H]^-$ formed upon DEA. In this study, which was accompanied by DFT calculations, it was shown that a sizable fraction of $[Val\text{-}H^+]^-$ formed upon DEA undergoes metastable decay. Furthermore it was also demonstrated that the metastable fragmentation channels observed for $[Val\text{-}H]^-$ that is formed by DEA are the same decay channels that are observed in PSD of the deprotonated ion $[Val\text{-}H^+]^-$ formed in MALDI. Thus, if the DEA fragments are formed *via* initial abstraction of hydrogen from the TNI and subsequent metastable decay, one expects to observe the same m/z ratios in both experiments. This is for instance the case for the fragment anion $m/z = 89$ that appears at the same mass in MALDI and DEA. As may be seen from Figs. 2 and 4 this fragment dominates the PSD spectra of both D-ribose and D-fructose. The measurements of DEA to D-ribose using the isotope labelled derivatives 1-^{13}C-R, 5-^{13}C-R and 1-D-R result partly in a shift to $m/z = 90$ similar to the PSD experiments described above. Fig. 7 compares the ion yield curves for the non-labelled D-ribose at $m/z = 89$ (shown at the top) with the ion yield curves obtained from the isotope labelled derivatives 5-^{13}C-R and 1-D-R at $m/z = 89$ and 90 in the electron energy range from close to zero eV to 3 eV. The ion yield is essentially the same for 1-^{13}C-R (not shown here) and for 1-D-R. In non-labelled D-ribose exclusively $m/z = 89$ is formed whereas in all isotope labelled molecules an additional signal at $m/z = 90$ is observed. The corresponding fragment anion is thus formed *via* two different pathways, i.e., with the negative charge remaining either on C1 or C5, similar to the reaction observed in PSD of $[R\text{-}H^+]^-$ in MALDI. The identical mass-to-charge ratio and the similar selectivity indicate that the $C_3H_5O_3^-$ fragment anion in DEA is in fact formed through metastable decay of the initially formed fragment $[R\text{-}H]^-$. Hence the ion is formed in DEA according to the following sequential reactions:

$$C_5H_{10}O_5 + e^- \rightarrow [C_5H_{10}O_5]^{\#-} \rightarrow [C_5H_9O_5]^- + H$$
$$\rightarrow C_3H_5O_3^-(89u) + 2CH_2O + H \quad (7)$$

A closer inspection of Fig. 7 shows that $C_3H_5O_3^-$ is generated from two overlapping resonances, one located at zero eV and the second at 0.6 eV. In 5-^{13}C-R the second resonance is completely shifted to $m/z = 90$ whereas the 0.6 eV signal remains at 89 in 1-D-R. This observation suggests that the TNI formed at 0.6 eV decays exclusively *via* abstraction of C1 and C2 according to an A-type cleavage. In contrast to that the TNI formed close to zero eV decays both through an A- and an X-type cross-ring cleavage. Thus there might actually be three different mechanisms behind the formation of the m/z ratio 89 in DEA. Alternatively this behaviour might be explained if DEA through the different resonances lead to H

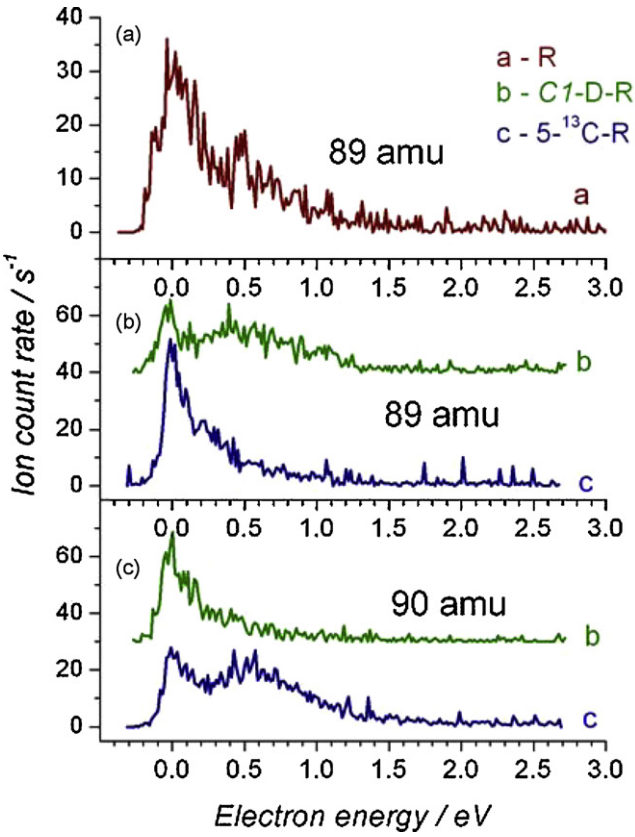

Fig. 7. Energy dependence of the $m/z = 89$ fragment anion, which is generated *via* electron attachment to D-ribose and subsequent metastable decay of $[R\text{-}H]^-$.

abstraction at different sites, which in turn leads to different fragmentation mechanisms. The comparatively low yield of $C_3H_5O_3^-$ can be due to the low internal energy of the precursor ion produced in DEA compared to MALDI. The decomposition reaction in DEA is solely triggered by the excess charge, thus the $[R\text{-}H^+]^-$ ion generated in MALDI possesses considerably higher internal energy leading to more efficient dissociation.

Another m/z ratio that is observed in both MALDI–PSD and in DEA is the m/z ratio 71. This anion is one of the dominant fragments in DEA but relatively weak in MALDI–PSD. In PSD it clearly results from a ^{0,2}A cross-ring cleavage as can be seen from the spectra in Fig. 4. In DEA on the other hand the reaction has been shown to proceed *via* a ^{3,5}X cleavage [26]. Hence the fragment at $m/z = 71$ is not the same in DEA to D-ribose and PSD of the deprotonated sugar.

Above we have concentrated on the metastable decay of the $[M-H]^-$ ion formed upon DEA. However it has also been shown that the interaction of the UV laser radiation with the organic-metal substrate in MALDI creates a number of photoelectrons [39–42] with energy below 1 eV. It was proposed that these electrons are captured by the matrix molecules resulting in further anionic products. In the present experiment the number of analyte molecules exceeds the number of matrix molecules and as electrons close to zero eV efficiently attach to the sugars D-ribose and D-fructose one can assume that electron attachment products contribute to the negative ion yield in ISD. If this is the case one would at least expect some of the same fragmentation products in MALDI–ISD and in DEA. The most dominant fragment anions in DEA have been observed at the m/z ratios 132, 101, 71 and 59. The ISD spectra of D-ribose are dominated by the m/z ratios 149, 129, 100, 71 and 58 with the most prominent fragment being the m/z ratio 71. In fact one of the dominating mechanisms behind the formation of the m/z ratio 71 in ISD is an X-type cross-ring cleavage as has also been shown to

be the case in DEA. However, other fragments that are observed in DEA appear only as minor contributions in ISD along with the dominant ISD peaks at the m/z ratios 129, 100 and 58, respectively. However, it should be kept in mind that the molecular anions $R^{\#-}$ generated in the DEA experiment decompose by unimolecular fragmentation, whereas multiple collisions occur within the desorption plume in MALDI. That is, when one assumes the generation of $R^{\#-}$ in MALDI due to the presence of photoelectrons, subsequent collisions with surrounding molecules could result in slightly different product ions as compared to DEA.

4. Conclusions

Metastable fragmentation of $[R\text{-}H^+]^-$ and $[Fru\text{-}H^+]^-$ results in water loss, but also considerable cross-ring cleavage with $C_3H_5O_3^-$ ($m/z = 89$) being the most dominant product anion. The use of isotope labelled D-ribose analogues showed that two different fragmentation pathways are operative corresponding either to an A-type cleavage or an X-type cleavage, respectively. This is in contrast to previous CID studies where only A-type cross-ring cleavage was proposed. We found that the heavier fragment anions at $m/z = 119$ and $m/z = 100$ generated *via* metastable decay exclusively arise from an X-type cleavage whereas the smaller fragment anions at $m/z = 89$ and 71 arise predominantly from an A-type cleavage. Fast fragmentation, which is observed in ISD, is dominated by X-type cleavage. The most dominant fragment in ISD is observed at $m/z = 71$ which consequently is not the same fragment ion as in PSD. Fragmentation of $[R\text{-}H^+]^-$ is compared to fragmentation of the transient molecular ion $R^{\#-}$ generated by electron attachment. Fragment ions observed in DEA to D-ribose are basically formed *via* loss of the same neutral fragments like deprotonated D-ribose. The fragment ion $C_3H_5O_3^-$ ($m/z = 89$) observed in DEA to R was identified to result from initial loss of hydrogen and subsequent metastable decay of $[R\text{-}H]^-$. However, the most dominant fragment ions in DEA are due to faster decomposition within several hundred nanoseconds (as in ISD), and a sequential reaction including an initial dehydrogenation can be excluded. The close resemblance of ISD mass spectra and DEA products suggests that photoelectrons can contribute to the ion yield. Further studies in this direction have to be performed.

Acknowledgements

This work is dedicated to our colleague and friend Zdenek Hermann who over many years pioneered many aspects in the field of chemical reaction dynamics in the gas phase and at surfaces. The authors acknowledge financial support from the Icelandic Centre for Research (RANNIS), the University of Iceland Research Fund, the Deutsche Forschungsgemeinschaft (DFG) and the Freie Universität Berlin. IB acknowledges support for a visit to Reykjavik by the COST action P9 (Radiation Damage in Biomolecular Systems, RADAM) of the European Science Foundation (ESF), and a PhD fellowship of the Studienstiftung des deutschen Volkes.

References

[1] D. Garozzo, G. Impallomeni, E. Spina, B.N. Green, T. Hutton, Carbohydr. Res. 221 (1991) 253.
[2] R.E. March, C.J. Stadey, Rapid Commun. Mass Spectrom. 19 (2005) 805.
[3] M.L. Coates, C.L. Wilkins, Anal. Chem. 59 (1987) 197.
[4] B. Spengler, J.W. Dolce, R.J. Cotter, Anal. Chem. 62 (1990) 1731.
[5] B. Spengler, D. Kirsch, R. Kaufmann, E. Jaeger, Rapid Commun. Mass Spectrom. 6 (1992) 105.
[6] B. Stahl, M. Steup, M. Karas, F. Hillenkamp, Anal. Chem. 63 (1991) 1463.
[7] H. Perreault, C.E. Costello, J. Mass Spectrom. 34 (1999) 184.
[8] J.C. Prome, H. Aurelle, D. Prome, A. Savagnac, Org. Mass Spectrom. 22 (1987) 6.
[9] J.W. Dallinga, W. Heerma, Biomed. Environ. Mass 18 (1989) 363.
[10] J.W. Dallinga, W. Heerma, Biol. Mass Spectrom. 20 (1991) 215.
[11] R.B. Cole, J.C. Tabet, C. Salles, J.C. Jallageas, J. Crouzet, Rapid Commun. Mass Spectrom. 3 (1989) 59.
[12] H. Krone, H.D. Beckey, Org. Mass Spectrom. 2 (1969) 427.
[13] H.D. Beckey, Int. J. Mass Spectrom. 2 (1969) 500.
[14] J.A. Carroll, L. Ngoka, C.G. Beggs, C.B. Lebrilla, Anal. Chem. 65 (1993) 1582.
[15] N.C. Polfer, J.J. Valle, D.T. Moore, J. Oomens, J.R. Eyler, B. Bendiak, Anal. Chem. 78 (2006) 670.
[16] G. Vall-Ilosera, M.A. Huels, M. Coreno, A. Kivimaki, K. Jakubowska, M. Stankiewicz, E. Rachlew, Chem. Phys. Chem. 9 (2008) 1020.
[17] I. Bald, Z. Deng, E. Illenberger, M.A. Huels, Phys. Chem. Chem. Phys. 8 (2006) 1215.
[18] Z.W. Deng, I. Bald, E. Illenberger, M.A. Huels, J. Chem. Phys. 127 (2007).
[19] J.-Y. Salpin, J. Tortajada, J. Mass Spectrom. 37 (2002) 379.
[20] J.-Y. Salpin, J. Tortajada, J. Phys. Chem. A 107 (2003) 2943.
[21] M. Alcami, A. Luna, O. Mo, M. Yanez, L. Boutreau, J. Tortajada, J. Phys. Chem. A 106 (2002) 2641.
[22] A. Fura, J.A. Leary, Anal. Chem. 65 (1993) 2805.
[23] S.M. Pimblott, J.A. LaVerne, Radic. Phys. Chem. 76 (2007) 1244.
[24] L. Sanche, Eur. Phys. J. D 35 (2005) 367.
[25] S. Ptasinska, S. Denifl, P. Scheier, T.D. Märk, J. Chem. Phys. 120 (2004) 8505.
[26] I. Bald, J. Kopyra, E. Illenberger, Angew. Chem. Int. Ed. 45 (2006) 4851.
[27] P. Sulzer, S. Ptasinska, F. Zappa, B. Mielewska, A.R. Milosavljevic, P. Scheier, T.D. Mark, I. Bald, S. Gohlke, M.A. Huels, E. Illenberger, J. Chem. Phys. 125 (2006) 044304.
[28] B. Domon, C.E. Costello, Glycoconj. J. 5 (1988) 397.
[29] M. Stano, H.D. Flosadottir, O. Ingolfsson, Rapid Commun. Mass Spectrom. 20 (2006) 3498.
[30] R. Balog, J. Langer, S. Gohlke, M. Stano, H. Abdoul-Carime, E. Illenberger, Int. J. Mass Spectrom. 233 (2004) 267.
[31] G. Luo, I. Marginean, A. Vertes, Anal. Chem. 74 (2002) 6185.
[32] V. Gabelica, E. Schulz, M. Karas, J. Mass Spectrom. 39 (2004) 579.
[33] B. Mulroney, J.B. Peel, J.C. Traeger, J. Mass Spectrom. 34 (1999) 544.
[34] J.-Y. Salpin, J. Tortajada, J. Mass Spectrom. 39 (2004) 930.
[35] B. Mulroney, J. Barrie Peel, J.C. Traeger, J. Mass Spectrom. 34 (1999) 856.
[36] J.A. Carroll, D. Willard, C.B. Lebrilla, Anal. Chim. Acta 307 (1995) 431.
[37] I. Baccarelli, F.A. Gianturco, A. Grandi, N. Sanna, R.R. Lucchese, I. Bald, J. Kopyra, E. Illenberger, J. Am. Chem. Soc. 129 (2007) 6269.
[38] H.D. Flosadottir, S. Denifl, F. Zappa, N. Wendt, A. Mauracher, A. Bacher, H. Jonsson, T.D. Maerk, P. Scheier, O. Ingolfsson, Angew. Chem. Int. Ed. 46 (2007) 8057.
[39] V. Frankevich, R. Knochenmuss, R. Zenobi, Int. J. Mass Spectrom. 220 (2002) 11.
[40] V.E. Frankevich, J. Zhang, S.D. Friess, M. Dashtiev, R. Zenobi, Anal. Chem. 75 (2003) 6063.
[41] R. Knochenmuss, Anal. Chem. 76 (2004) 3179.
[42] M. Dashtiev, V. Frankevich, R. Zenobi, J. Phys. Chem. A 110 (2006) 926.